nature geoscience

LETTERS

PUBLISHED ONLINE: 9 FEBRUARY 2015 | DOI: 10.1038/NGEO2353

Aerosol forcing of the position of the intertropical convergence zone since AD 1550

Harriet E. Ridley[1]*, Yemane Asmerom[2], James U. L. Baldini[1], Sebastian F. M. Breitenbach[3], Valorie V. Aquino[4], Keith M. Prufer[4], Brendan J. Culleton[5], Victor Polyak[2], Franziska A. Lechleitner[3], Douglas J. Kennett[5], Minghua Zhang[6], Norbert Marwan[7], Colin G. Macpherson[1], Lisa M. Baldini[1], Tingyin Xiao[6], Joanne L. Peterkin[1], Jaime Awe[8] and Gerald H. Haug[3]

The position of the intertropical convergence zone is an important control on the distribution of low-latitude precipitation. Its position is largely controlled by hemisphere temperature contrasts[1,2]. The release of aerosols by human activities may have resulted in a southward shift of the intertropical convergence zone since the early 1900s (refs 1,3–6) by muting the warming of the Northern Hemisphere relative to the Southern Hemisphere over this interval[1,7,8], but this proposed shift remains equivocal. Here we reconstruct monthly rainfall over Belize for the past 456 years from variations in the carbon isotope composition of a well-dated, monthly resolved speleothem. We identify an unprecedented drying trend since AD 1850 that indicates a southward displacement of the intertropical convergence zone. This drying coincides with increasing aerosol emissions in the Northern Hemisphere and also marks a breakdown in the relationship between Northern Hemisphere temperatures and the position of the intertropical convergence zone observed earlier in the record. We also identify nine short-lived drying events since AD 1550 each following a large volcanic eruption in the Northern Hemisphere. We conclude that anthropogenic aerosol emissions have led to a reduction of rainfall in the northern tropics during the twentieth century, and suggest that geographic changes in aerosol emissions should be considered when assessing potential future rainfall shifts in the tropics.

Intertropical convergence zone (ITCZ) position largely controls low-latitude seasonal rainfall distribution. Relative ITCZ position is strongly influenced by hemispheric temperature contrasts and subsequent atmospheric restructuring, which draw the ITCZ towards the warmer hemisphere[1,2,5]. Indeed, considerable proxy evidence links Northern Hemisphere temperature (NHT) to low-latitude rainfall throughout the Holocene[9–11]. However, since 1900, limited instrumental evidence suggests a southward shift in ITCZ position[3,5], a trend possibly driven by asymmetrical hemispheric warming due to the relative cooling effect of anthropogenic sulphate aerosols in the Northern Hemisphere, but that could also arise from undetected natural variability. Climate models have attempted to assess the relative contributions of greenhouse gases (GHGs) and aerosols to ITCZ displacement with contradictory results[1,7]. Limited long-term instrumental climate records from low latitudes complicate detecting climate shifts attributable to anthropogenic influences, and consequently future precipitation projections remain ambiguous[12]. Furthermore, chronological uncertainties associated with low-latitude rainfall proxy records prevent establishing robust links between low-latitude rainfall amount and atmospheric aerosol distributions at a suitable resolution. Here, we discuss an exceptionally well-dated, monthly scale stalagmite rainfall record covering 456 years from AD 1550 to 2006, thus covering the critical transition into the current warm period with unprecedented detail and providing much needed evidence to support modelling work.

A stalagmite identified as YOK-G was obtained from Yok Balum Cave in southern Belize (16° 12′ 30.780″ N, 89° 4′ 24.420″ W; 336 metres above sea level; Supplementary Fig. 7). This site is near the northernmost extent of the ITCZ, a remarkably sensitive location for reconstructing even minor variations in ITCZ position. The cave was undisturbed before 2005 and is characterized by a stable low-p_{CO_2} atmosphere, consistent year-round temperatures (22.3 °C ± 0.5), and high relative humidity (>95%; Supplementary Figs 17 and 18). The cave is remote and located below steep, dense forest that is unsuitable for farming or mechanized logging, minimizing potential past human interferences at the site. Outside air temperature varies only between 20 °C (December to February) and 24 °C (June to August). However, rainfall is distinctly seasonal, ranging from 40–70 mm per month in the peak dry season (February to April) to 400–700 mm per month during the peak wet season (June to September) owing to seasonal ITCZ and associated trade wind migrations that track the thermal equator[13]. Evapotranspiration surpasses precipitation during the dry season[14], reducing effective rainfall and water input to the karst system. Stalagmite YOK-G was collected in 2006 and is 1,090 mm tall, but only the top 365 mm are discussed here. A total of 3,648 carbonate samples were collected by milling continuously at 100 μm increments along the central growth axis, and carbon and oxygen stable isotope ratios were determined using a Thermo MAT 253 gas source mass spectrometer.

Annual carbon isotope ratio ($\delta^{13}C$) cycles apparent throughout most of the record provide exceptional chronological control. The uppermost 8 mm milled at a 100 μm spatial resolution did not reveal $\delta^{13}C$ cycles, which prevented counting cycles back from the date of collection. The $\delta^{13}C$ cycle chronology is instead anchored to the first

[1]Department of Earth Sciences, University of Durham, Durham DH1 3LE, UK. [2]Department of Earth and Planetary Sciences, University of New Mexico, Albuquerque, New Mexico 87106, USA. [3]Department of Earth Science, Eidgenössische Technische Hochschule (ETH), CH-8092 Zürich, Switzerland. [4]Department of Anthropology, University of New Mexico, Albuquerque, New Mexico 87106, USA. [5]Department of Anthropology, The Pennsylvania State University, University Park, Pennsylvania 16802, USA. [6]Institute for Terrestrial and Planetary Atmospheres, School of Marine and Atmospheric Sciences, Stony Brook, New York 11794-5000, USA. [7]Potsdam Institute for Climate Impact Research, PO Box 60 12 03, 14412 Potsdam, Germany. [8]Department of Anthropology, Northern Arizona University, Flagstaff, Arizona 86001, USA. *e-mail: h.e.ridley@durham.ac.uk

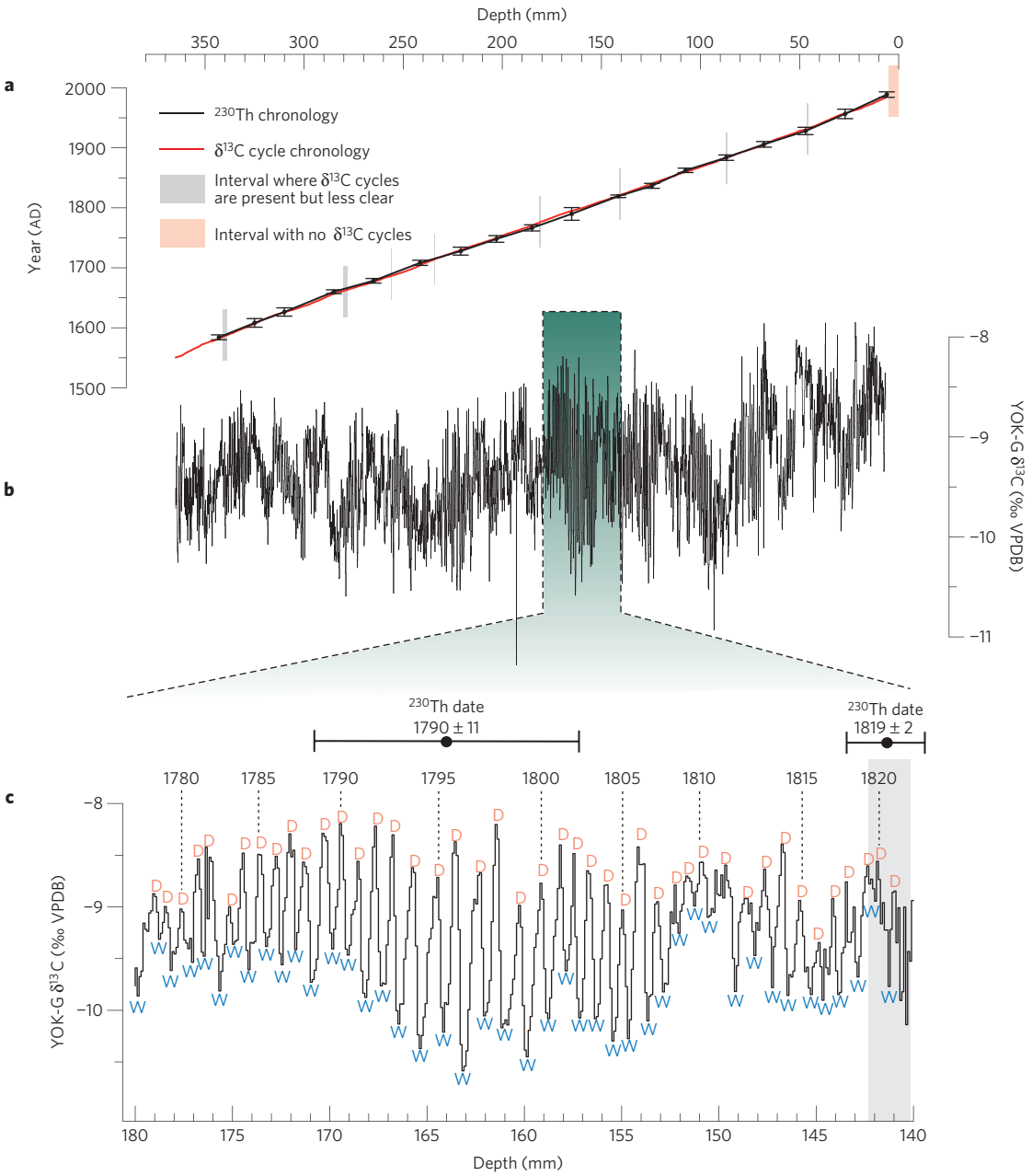

Figure 1 | YOK-G $\delta^{13}C$ record and chronology. a, ^{230}Th dates with 2σ errors (black line) and $\delta^{13}C$ cycle chronology (red line) fitted with cubic splines. Shaded grey rectangles indicate intervals where the $\delta^{13}C$ cycles are present but less clear. The shaded pink rectangle indicates the interval (1983–2006) where $\delta^{13}C$ cycles are absent. ^{230}Th dates verified the $\delta^{13}C$ cycle count chronology, but are independent of the final chronological model. **b**, The entire YOK-G $\delta^{13}C$ record against depth. **c**, An expanded view of 40 mm of growth illustrating $\delta^{13}C$ annual cycles with peak wet- (W) and dry- (D) season $\delta^{13}C$ values identified.

evidence of atmospheric 'bomb' radiocarbon in 1955 (Supplementary Information and Supplementary Fig. 14). Higher-resolution (25 μm; weekly scale) re-milling over the top 8 mm also failed to detect $\delta^{13}C$ cycles (Supplementary Fig. 12), strongly suggesting that no $\delta^{13}C$ cycles exist in the most recent part of the stalagmite. If 2006 is used as the cessation of sample growth (due to collection), the calculated growth rate for this interval deviates significantly from the nearly uniform growth rate for the preceding ~500 years. This suggests that either: carbonate precipitation slows down at some point since 1984; the sample stopped growing earlier than the date of collection; or a combination of both. This short interval (from 1984 to 2006) is therefore not included in the discussion owing to increased chronological uncertainty. X-ray diffraction results indicate that YOK-G is entirely aragonitic, which, owing to its high capacity for uranium inclusion, permits the construction of a precise ^{230}Th chronology (Fig. 1 and Supplementary Table 1). Eighteen high-precision ^{230}Th dates obtained using multi-collector inductively coupled plasma mass spectrometry confirm that the $\delta^{13}C$ cycle-derived model is robust (Fig. 1). Between AD 1550 and 1983 YOK-G grew continuously with a mean growth rate of 0.82 mm yr^{-1}.

Here we use the YOK-G $\delta^{13}C$ record as a palaeorainfall proxy. Stalagmite $\delta^{13}C$ in low-latitude regions not experiencing temporal shifts in vegetation type (for example, shifts from C3 to C4 vegetation) largely reflects effective rainfall amount and the hydrology of the drip feeding the stalagmite. Dry intervals promote: prior carbonate precipitation (due to lower groundwater flow

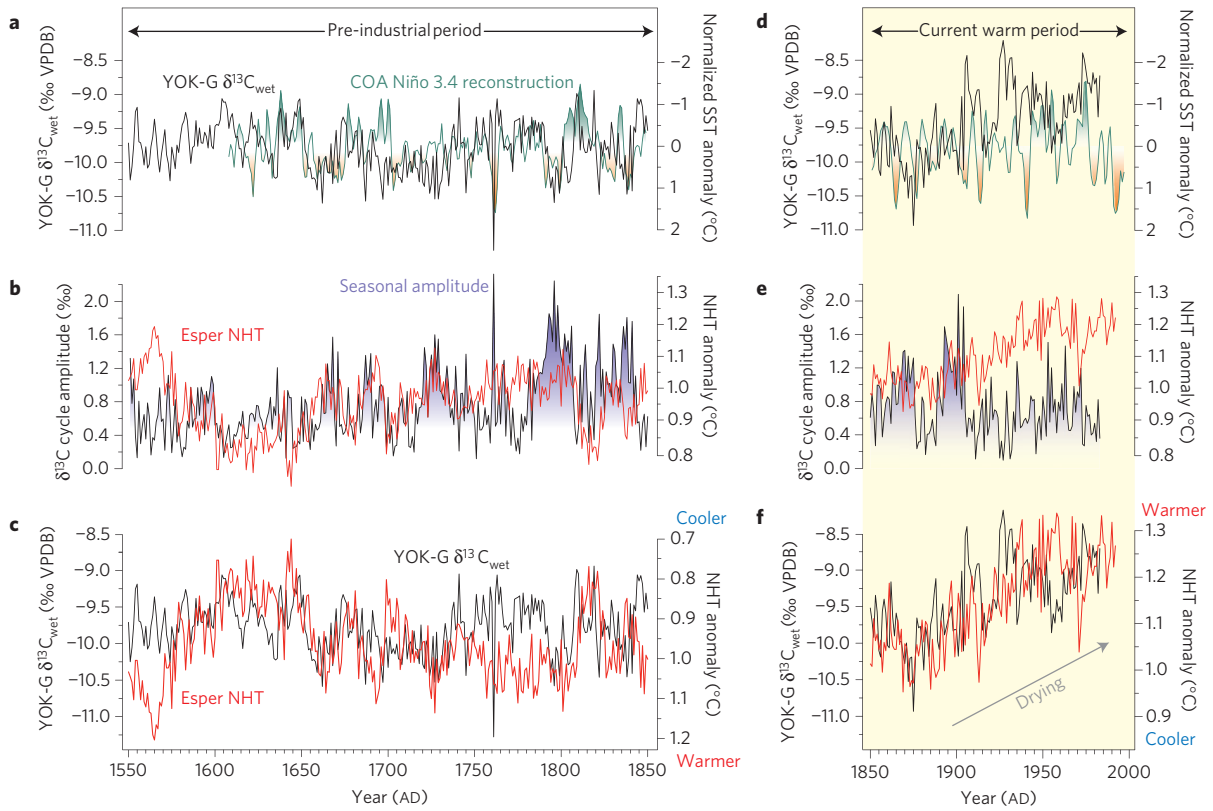

Figure 2 | YOK-G $\delta^{13}C$ record. a, YOK-G wet season $\delta^{13}C$ record and the Niño 3.4 Center of Action (COA) reconstruction[18] for the period 1550–1850. **b**, Seasonality defined by the amplitude of each annual $\delta^{13}C$ from peak wet season to peak dry season and NHT from the Esper reconstruction (ref. 19) for the period 1550–1850. **c**, YOK-G $\delta^{13}C_{wet}$ against NHT for the period 1550–1850. **d**, The same as in **a** but for the industrial interval of the record, 1851–1983. **e**, The same as in **b** but for the period 1851–1983. **f**, The same as in **c** but for the period 1851–1983.

rates); increased bedrock carbon contributions; and reduced soil bioproductivity, all contributing to a more positive $\delta^{13}C$. Conversely, wetter conditions result in more negative $\delta^{13}C$ (see Supplementary Information). This interpretation is supported by the remarkable, demonstrably annual $\delta^{13}C$ cycle reflecting seasonal water recharge conditions, as well as by interpretations of other Belizean stalagmite $\delta^{13}C$ records as reflecting rainfall, notably ref. 15, linking pronounced $\delta^{13}C$ increases to El Niño-related rainfall reductions, and ref. 16 linking $\delta^{13}C$ shifts over the past 3,300 years to rainfall. We note that these two studies represent the two published speleothem records from cave sites closest to Yok Balum Cave (ATM Cave, ~100 km to the north, and Macal Chasm, ~80 km to the north), and that both used $\delta^{13}C$ as a palaeorainfall proxy (Supplementary Fig. 4). The similarity between the YOK-G $\delta^{13}C$ record and the Cariaco Basin record ITCZ rainfall record[10] also strongly supports this interpretation. We stress that $\delta^{18}O$ is also an extremely useful complementary rainfall proxy[17] (see Supplementary Information), but we believe that under the conditions at our site, $\delta^{13}C$ is more sensitive to subtle shifts in recharge.

Both wet- and dry-season $\delta^{13}C$ values ($\delta^{13}C_{wet}$ and $\delta^{13}C_{dry}$) are clearly distinguishable in the YOK-G record (Fig. 1c), providing a rare opportunity to isolate rainfall amount during specific seasons at a low-latitude site. YOK-G $\delta^{13}C_{wet}$ and the NINO3.4 Center of Action sea surface temperature (SST) reconstruction[18] are anticorrelated ($r = -0.3$, $p < 0.001$ with a nine-year moving average applied) during the pre-industrial period (1550–1850), suggesting that eastern equatorial Pacific SST exerted a significant control on Belizean rainfall (Fig. 2a). In addition, a weak but significant negative relationship ($r = -0.19$, $p < 0.001$) exists between the NHT reconstruction in ref. 19 and $\delta^{13}C_{wet}$ during the pre-industrial interval of the record (Fig. 2c). This suggests that a warmer Northern Hemisphere tends to draw the ITCZ to a more northerly position, consistent with the results of numerous previous studies[7,10]. No relationship exists between $\delta^{13}C_{dry}$ and NHT ($r = 0.05$, $p = 0.43$), again consistent with the interpretation of YOK-G $\delta^{13}C_{wet}$ as an ITCZ rainfall proxy. Elevated NHT tended to cause a more seasonal rainfall distribution (greater seasonality) during the pre-industrial portion of the YOK-G record ($r = 0.32$, $p < 0.001$ with nine-year moving average applied; Fig. 2b).

However, post-1850 all of the $\delta^{13}C$ data (mean annual, wet season and dry season) strongly suggest a steady drying trend coinciding with increasing NHT, suggesting a pronounced reversal in the relationship between NHT and ITCZ position (Fig. 3). In addition, post-1850 YOK-G annual mean $\delta^{13}C$ tracks trends in global GHG concentrations and anthropogenic aerosol emissions (Fig. 4). This indicates a southward ITCZ migration despite increasing NHT.

The timing of this relationship reversal suggests an anthropogenic link. Recent research highlights the competing effects of GHG and anthropogenic aerosols on low-latitude rain belts, with GHG increases believed to force the ITCZ to the north, and aerosols to the south[5,7]. Modelling studies suggest that a heterogeneous regional cooling effect induced by Northern Hemisphere mid-latitude anthropogenic aerosol emissions drove the southward migration of the ITCZ over recent decades[1,3,4,7], leading to drought in the Sahel[8,20] and parts of monsoonal Asia[21,22]. The rainfall decreases implied by the YOK-G record closely follow patterns of regional industrialization and aerosol emissions in North America and western Europe since ~1880 (Fig. 4 and Supplementary Fig. 24). Peak US aerosol production during the period 1970–1990 is estimated to have had a direct radiative forcing of $-6\ W\ m^{-2}$ over the central and eastern US resulting in relative cooling of 0.5–1.0 °C (ref. 23). Cooling over the North Atlantic

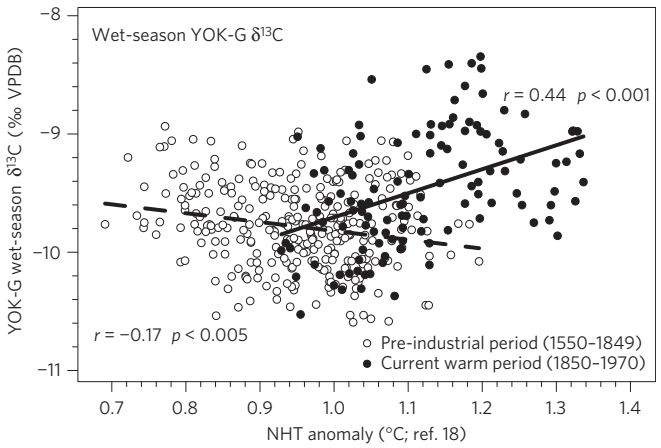

Figure 3 | Scatterplot of YOK-G $\delta^{13}C_{wet}$ versus NHT from the Esper reconstruction. Data for the pre-industrial period (1550–1849; open circles) show weak significant negative correlation ($r = -0.19$, $p < 0.005$), and data for the current warm period (1850–1983; black filled circles) exhibit a switch to a significant positive correlation ($r = 0.43$, $p < 0.001$).

region modifies atmospheric circulation to accommodate cross-equatorial thermal contrasts and subsequently drives the ITCZ southward[24].

The YOK-G record also illustrates that very similar ITCZ repositioning occurred following large Northern Hemisphere volcanic eruptions that injected sulphate aerosols into the atmosphere. These affected the ITCZ through a similar mechanism as anthropogenic aerosols, causing preferential Northern Hemisphere cooling, southward ITCZ migration, and consequently drying in Belize. Particularly noteworthy is the coincidence of the large and climatologically significant Laki eruption (1783–1784) with the height of the largest pre-industrial drought in Belize since AD 1550, evident in both the YOK-G and local historical records. The Laki eruption produced a peak estimated direct radiative forcing in August 1783 of -5.5 W m^{-2} in the Northern Hemisphere[25], similar to the magnitude of the anthropogenic aerosol peak during 1970–1990 (-6 W m^{-2}), and resulted in comparable drying in Belize. However, we note that the direct climate effects attributable to the Laki eruption were unlikely to have lasted more than three years[25], so the 1783 eruption may have exacerbated or prolonged the 1765–1800 drought but was not the principal driver. Southern Hemisphere volcanic eruptions, including those at low southerly latitudes, seem to force the ITCZ to the north. Most notable of these is the Tambora eruption in 1815, associated with increased Belizean rainfall the following year (Fig. 4). Of the nine largest Northern Hemisphere eruptions identified in the Greenland Ice Sheet Project 2 (GISP2) ice-core sulphate record and the historical record since 1550 (ref. 26), all are associated with drying in Belize; conversely, all three large Southern Hemisphere eruptions are associated with increased rainfall at

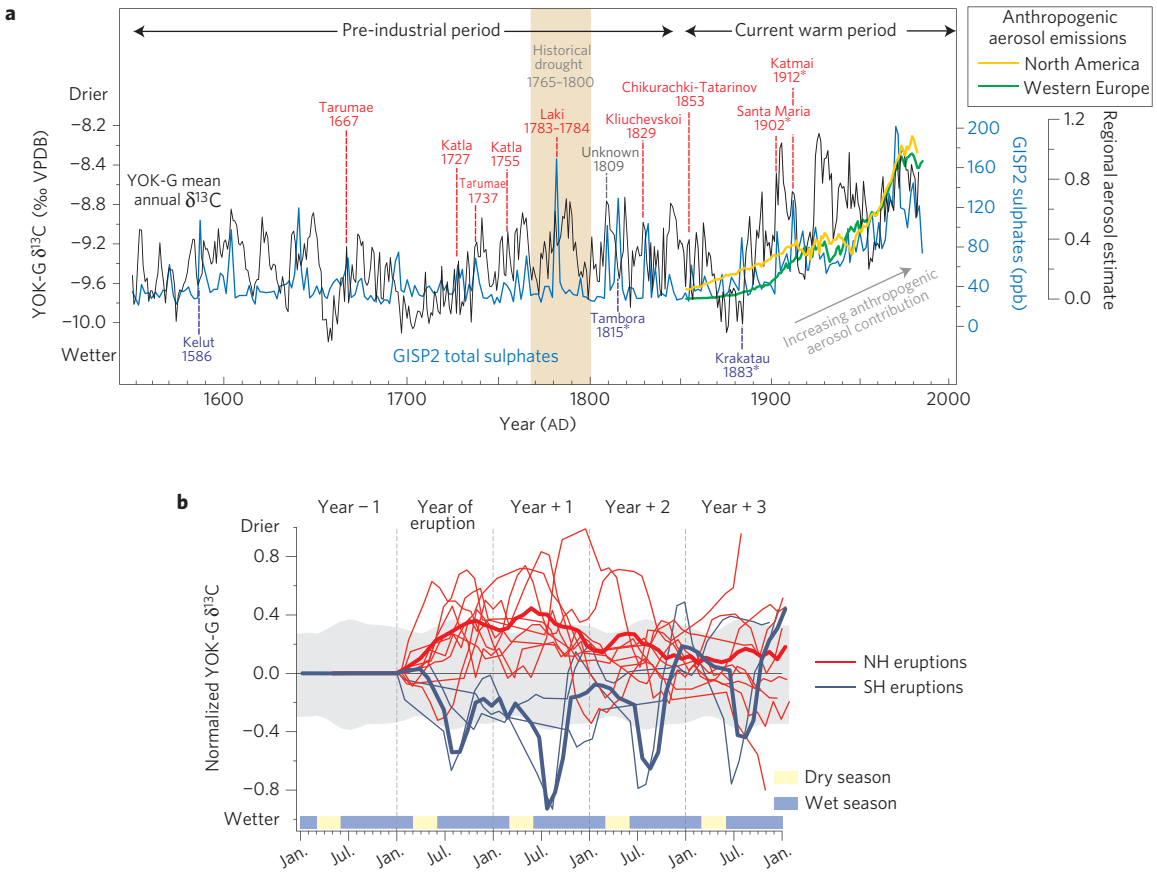

Figure 4 | Annual mean YOK-G $\delta^{13}C$ and links to sulphate aerosols. a, Annual mean $\delta^{13}C$ (black) and GISP2 total sulphate record (blue)[26]. Aerosol production estimated using CO_2 emissions relative to 1992 levels[29,30] for Europe (green) and North America (yellow). Major (volcanic explosivity index (VEI) ≥ 5) Northern Hemisphere eruptions (red) and Southern Hemisphere eruptions (blue) are marked. Dashed lines designate conventionally accepted eruption date. Asterisks highlight VEI ≥ 6 eruptions. **b**, Climate response to Northern Hemisphere (NH) and Southern Hemisphere (SH) eruptions implied by YOK-G $\delta^{13}C$ values (normalized to monthly means in the year preceding the eruption). Shading denotes the one sigma standard deviation from the monthly mean values over the entire record. Thick lines represent mean $\delta^{13}C$ response to Northern Hemisphere and Southern Hemisphere eruptions.

our site. Specifically, the YOK-G record indicates that Northern Hemisphere eruptions result in substantially elevated $\delta^{13}C_{dry}$, and we suggest that this reflects a longer dry season caused by delayed onset of the summer wet season. Our data suggest that Northern Hemisphere eruptions shortened the duration of the wet season, and Southern Hemisphere eruptions extended wet-season duration. The record provides compelling evidence that stratospheric sulphate aerosol injections associated with explosive volcanism resulted in short-lived ITCZ migration (Fig. 4). This result is consistent with recent modelling results suggesting that large volcanic eruptions that inject aerosols into the Northern Hemisphere cause the ITCZ to migrate to the south, whereas Southern Hemisphere eruptions push the ITCZ to the north[27], and with historical records suggesting reduced Nile discharge following the 1783 Laki eruption[28]. Similarly, continuous Northern Hemisphere anthropogenic aerosol emissions during the twentieth century drove sustained southward ITCZ repositioning.

The monthly resolved YOK-G $\delta^{13}C$ rainfall record provides the strongest proxy evidence available that recent droughts in the northern tropics are attributable to extra-tropical anthropogenic forcing. Rather than being a cyclic natural phenomenon, sustained rainfall reductions in Belize occurred only after atmospheric aerosols increased following regional industrialization in the Northern Hemisphere. The record also indicates that similar (albeit shorter lived) ITCZ repositioning occurred in response to sulphate aerosol forcing associated with large Northern Hemisphere volcanic eruptions. Future modelling should focus on determining how shifts in regional aerosol emission rates might affect ITCZ position. This is particularly relevant to industrializing regions where large populations are dependent on seasonal rainfall.

Methods

Stable isotope analysis. Stalagmite YOK-G was continuously milled at 0.1 mm steps along the central growth axis using a computer-controlled ESI/New Wave Micromill with a standard 0.8 mm tungsten carbide drill bit. Samples were milled to specifications of 0.1 mm width, 10 mm length and 1 mm depth, with the long axis parallel to growth layers. Stable isotope analysis was conducted at Durham University using a Thermo-Finnigan (now Thermo Fisher Scientific) MAT 253 Isotope-Ratio Mass Spectrometer with a Gasbench II (external precision of about 0.05–0.10‰). Each analysis utilized 220–250 µg of sample powder. About 50 speleothem carbonate samples were loaded for each run. Carbonate samples were dissolved in 10 drops of orthophosphoric acid (H_3PO_4) under a helium (grade 5) atmosphere. The solution was left to digest at 50 °C for two hours. The resultant gas mixture (CO_2 and He) was introduced to a gas chromatographic column and the CO_2 separated from the gas mixture. After passing the second water trap the analyte was admitted to the mass spectrometer. Each sample run included 14 reference standards of IAEA (International Atomic Energy Agency) international reference materials NBS18 (carbonatite), NBS19 (limestone) and LS VEC (lithium carbonate) and an additional internal laboratory standard. Normalizations and corrections were made to NBS19 and LS VEC. $^{13}C/^{12}C$ ratios are reported relative to the Vienna PeeDee Belemnite (VPDB) standard.

Chronology. Uranium-series (^{230}Th) dating of powders was performed at the University of New Mexico Radiogenic Isotope Laboratory. Milled powder samples (20–120 mg) and a drip water sample (13.3 g) were spiked with a solution containing ^{229}Th, ^{233}U and ^{236}U. Uranium and thorium were separated using anion chemistry and analysed on a Thermo Neptune multi-collector inductively coupled plasma mass spectrometer. Improved half-life values for ^{230}Th and ^{234}U were applied to these age results (see Supplementary Information). Drip water and YOK-G carbonate powders extracted at 0.5 and 1.0 mm from the stalagmite top (years AD 2006 and 2004) were used to establish that stalagmite YOK-G detrital thorium has a high initial $^{230}Th/^{232}Th$. This high initial value was found to be inversely correlated to ^{232}Th concentration such that initial $^{230}Th/^{232}Th_{atomic}$ (ppm) = 323.67(X) − 0.269, where X is the concentration of ^{232}Th in picograms per gram, and the calculated initial $^{230}Th/^{232}Th_{atomic}$ (ppm) has an assumed ±10% absolute error. These high initial values result in higher absolute errors on ^{230}Th ages but do not significantly affect age results older than AD 1800.

Incremental accelerator mass spectrometry ^{14}C on the upper 48 mm of YOK-G was performed to help constrain growth rates over the past 50 years. Samples were milled along visible growth increments offset from the stable isotope milling track. Accelerator mass spectrometry ^{14}C analyses were made on a modified National Electrostatics Corporation compact spectrometer and all ^{14}C ages were corrected for mass-dependent fractionation. Identification of the initial part of the atmospheric bomb spike at AD 1955 provided both an independent confirmation of the accuracy of the top ^{230}Th dates and a date (1955) with which to anchor the annual $\delta^{13}C$ cycle chronology. Carbon cycles were counted from this marker. Within the carbon cycles, higher $\delta^{13}C$ values correspond with the end of the dry season (April) when the karst is most extensively drained and lower $\delta^{13}C$ values represent the peak of the wet season (July). The carbon cycle chronology is consistent with the ^{230}Th chronology and is never outside the errors associated with any particular ^{230}Th date. The $\delta^{13}C$ cycles therefore provide an accurate sub-seasonally resolved chronology.

Received 1 September 2014; accepted 2 January 2015; published online 9 February 2015

References

1. Hwang, Y. T., Frierson, D. M. W. & Kang, S. M. Anthropogenic sulfate aerosol and the southward shift of tropical precipitation in the late 20th century. *Geophys. Res. Lett.* **40,** 2845–2850 (2013).
2. Broccoli, A. J., Dahl, K. A. & Stouffer, R. J. Response of the ITCZ to Northern Hemisphere cooling. *Geophys. Res. Lett.* **33,** L01702 (2006).
3. Rotstayn, L. D. & Lohmann, U. Tropical rainfall trends and the indirect aerosol effect. *J. Clim.* **15,** 2103–2116 (2002).
4. Chang, C. Y., Chiang, J. C. H., Wehner, M. F., Friedman, A. R. & Ruedy, R. Sulfate aerosol control of tropical Atlantic climate over the twentieth century. *J. Clim.* **24,** 2540–2555 (2011).
5. Zhang, X. *et al.* Detection of human influence on twentieth-century precipitation trends. *Nature* **448,** 461–465 (2007).
6. Lu, H. Y. *et al.* Variation of East Asian monsoon precipitation during the past 21 k.y. and potential CO_2 forcing. *Geology* **41,** 1023–1026 (2013).
7. Friedman, A. R., Hwang, Y. T., Chiang, J. C. H. & Frierson, D. M. W. Interhemispheric temperature asymmetry over the twentieth century and in future projections. *J. Clim.* **26,** 5419–5433 (2013).
8. Booth, B. B. B., Dunstone, N. J., Halloran, P. R., Andrews, T. & Bellouin, N. Aerosols implicated as a prime driver of twentieth-century North Atlantic climate variability. *Nature* **484,** 228–232 (2012).
9. Dykoski, C. A. *et al.* A high-resolution, absolute-dated Holocene and deglacial Asian monsoon record from Dongge Cave, China. *Earth Planet Sci. Lett.* **233,** 71–86 (2005).
10. Haug, G. H., Hughen, K. A., Sigman, D. M., Peterson, L. C. & Rohl, U. Southward migration of the intertropical convergence zone through the Holocene. *Science* **293,** 1304–1308 (2001).
11. Zhang, P. Z. *et al.* A test of climate, sun, and culture relationships from an 1810-year chinese cave record. *Science* **322,** 940–942 (2008).
12. Diffenbaugh, N. S. & Field, C. B. Changes in ecologically critical terrestrial climate conditions. *Science* **341,** 486–492 (2013).
13. Poveda, G., Waylen, P. R. & Pulwarty, R. S. Modern climate variability in northern South America and southern Mesoamerica. *Palaeogeogr. Palaeoclimatol.* **234,** 3–27 (2006).
14. Heyman, W. D. & Kjerfve, B. Hydrological and oceanographic considerations for integrated coastal zone management in southern Belize. *Environ. Manage.* **24,** 229–245 (1999).
15. Frappier, A., Sahagian, D., Gonzalez, L. A. & Carpenter, S. J. El Niño events recorded by stalagmite carbon isotopes. *Science* **298,** 565 (2002).
16. Webster, J. W. *et al.* Stalagmite evidence from Belize indicating significant droughts at the time of Preclassic Abandonment, the Maya Hiatus, and the Classic Maya collapse. *Palaeogeogr. Palaeoclimatol.* **250,** 1–17 (2007).
17. Kennett, D. J. *et al.* Development and disintegration of Maya political systems in response to climate change. *Science* **338,** 788–791 (2012).
18. Wilson, R. *et al.* Reconstructing ENSO: The influence of method, proxy data, climate forcing and teleconnections. *J. Quat. Sci.* **25,** 62–78 (2010).
19. Esper, J., Cook, E. R. & Schweingruber, F. H. Low-frequency signals in long tree-ring chronologies for reconstructing past temperature variability. *Science* **295,** 2250–2253 (2002).
20. Kawase, H. *et al.* Physical mechanism of long-term drying trend over tropical North Africa. *Geophys. Res. Lett.* **37,** L09706 (2010).
21. Bollasina, M. A., Ming, Y. & Ramaswamy, V. Anthropogenic aerosols and the weakening of the South Asian summer monsoon. *Science* **334,** 502–505 (2011).
22. Lau, K. M., Kim, M. K. & Kim, K. M. Asian summer monsoon anomalies induced by aerosol direct forcing: The role of the Tibetan Plateau. *Clim. Dynam.* **26,** 855–864 (2006).
23. Leibensperger, E. M. *et al.* Climatic effects of 1950:2050 changes in US anthropogenic aerosols: Part 1: Aerosol trends and radiative forcing. *Atmos. Chem. Phys.* **12,** 3333–3348 (2012).
24. Tokinaga, H. & Xie, S. P. Weakening of the equatorial Atlantic cold tongue over the past six decades. *Nature Geosci.* **4,** 222–226 (2011).

25. Highwood, E. J., Stevenson, D. S., Highwood, E. J. & Stevenson, D. S. Atmospheric impact of the 1783–1784 Laki eruption: Part II - climatic effect of sulphate aerosol. *Atmos. Chem. Phys.* **3,** 1177–1189 (2003).
26. Zielinski, G. A. *et al.* Record of volcanism since 7000-BC from the GISP2 Greenland ice core and implications for the volcano-climate system. *Science* **264,** 948–952 (1994).
27. Haywood, J. M., Jones, A., Bellouin, N. & Stephenson, D. Asymmetric forcing from stratospheric aerosols impacts Sahelian rainfall. *Nature Clim. Change* **3,** 660–665 (2013).
28. Oman, L., Robock, A., Stenchikov, G. L. & Thordarson, T. High-latitude eruptions cast shadow over the African monsoon and the flow of the Nile. *Geophys. Res. Lett.* **33,** L18711 (2006).
29. Marland, G., Andres, R. J. & Boden, T. A. in *Trends '93: A Compendium of Data on Global Change* (eds Boden, T. A., Kaiser, D. P., Sepanski, R. J. & Stoss, F. W.) 505–584 (Oak Ridge Nat. Lab., 1994).
30. Robertson, A. *et al.* Hypothesized climate forcing time series for the last 500 years. *J. Geophys. Res.* **106,** 14783–14803 (2001).

Acknowledgements

This research was supported by funding from: the European Research Council (grant 240167 to J.U.L.B.); National Science Foundation of the United States (grant BCS-0620445 to K.M.P., grant HSD-0827305 to K.M.P. and Y.A., grant HSD-0827275 to D.J.K., and grant BCS-0940744 to D.J.K. and M.Z.); the Alphawood Foundation (grant to K.M.P.); the Schweizer National Fund, Sinergia (grant CRSI22 132646/1 to S.F.M.B.). Research permits were issued by the Belize Institute of Archaeology. Hydromet Belize are thanked for meteorological data.

Author contributions

H.E.R. produced the stable isotope record with assistance from C.G.M. and J.L.P. Y.A., V.P. and V.V.A. were responsible for developing the uranium-series chronology. D.J.K. and B.J.C. performed radiocarbon analyses. H.E.R., K.M.P. and J.U.L.B. contributed significantly to fieldwork. M.Z. and T.X. performed GHCN analyses. F.A.L. and S.F.M.B. performed high-resolution stable isotope reanalyses. H.E.R. and J.U.L.B. wrote the manuscript. J.A. contributed to logistics associated with fieldwork. All named co-authors contributed to the project, discussed manuscript ideas and approved the final manuscript.

Additional information

Supplementary information is available in the online version of the paper. Reprints and permissions information is available online at www.nature.com/reprints. Correspondence and requests for materials should be addressed to H.E.R.

Competing financial interests

The authors declare no competing financial interests.